THE ASTROPHYSICAL JOURNAL, 198:527–536, 1975 June 15

AN H I STUDY OF Scd GALAXIES

G. S. SHOSTAK
National Radio Astronomy Observatory,* Charlottesville, Virginia
Received 1974 November 12

ABSTRACT

H I line profiles, together with derived redshifts and integral properties, are presented for 46 Scd galaxies. The profile shapes are quite regular, with a double-peaked structure characteristic of galaxies with flat rotation curves. The ratios $M_{\rm H\,I}/M_T$ and $M_{\rm H\,I}/L_{\rm pg}$, which are known to vary with Hubble type, have observed dispersions of ± 80 percent within this classification, with intrinsic dispersions being probably less than ± 50 percent. This establishes that integral property ratios are substantially homogeneous within the Scd classification.

No indication of H I optical-depth effects with inclination is observed.

Evidence is presented that distances derived solely from redshifts have an average uncertainty of < 0.8 mag in the distance modulus.

Subject headings: galaxies, motion in — galaxies, stellar content of — redshifts — 21-cm radiation

I. INTRODUCTION

H I line profiles are presently available for several hundred galaxies. The majority of these objects have been observed at Nançay and Green Bank, the most extensive compendia of the data being those of Balkowski (1973) and Roberts (1969). These works have covered the Hubble sequence from the early spirals to the irregulars, and have sought to establish correlations of integral properties such as hydrogen mass $M_{\rm H\,I}$, total mass M_T, and photographic luminosity $L_{\rm pg}$, or ratios of these properties, with Hubble type. The most firmly established correlations show that the fractional H I mass, $M_{\rm H\,I}/M_T$, and the ratio of H I mass to light, $M_{\rm H\,I}/L_{\rm pg}$, increase as we go from early to later type. The progressive increase of these ratios implies a continuity of the Hubble sequence. It also suggests that it may be possible to deduce physical explanations of the diverse morphologies of the sequence from their differing integral properties.

Clearly, if Hubble type is one, or the only one, of the parameters determining integral property ratios, then a reduction in the dispersion of these ratios should obtain for galaxies of a given type. Rogstad and Shostak (1972) used aperture-synthesis techniques to study several Scd galaxies in two dimensions. On the basis of data collected for five galaxies, they concluded that all the objects had similar rotation curves, implying similar radial total mass functions and mass-to-light ratios. The rotation curves were essentially flat beyond 0.6 times the Holmberg (1958) radius. Furthermore, their H I distributions scaled with optical radius, 80 percent of the observable hydrogen mass being contained within 1 Holmberg radius. Integral property ratios were nearly the same for all objects; but since these quantities depend on accurate values for distances and inclinations, this observation was not firmly established. Data from a much larger sample of galaxies were required to confirm the homogeneity of properties within the Scd classification. The present study was motivated by the desire to establish this homogeneity, thereby relating morphological type to physical parameters. A study of the integral properties alone requires only global H I line profiles, and these can be obtained relatively quickly using a single-dish telescope.

For this study, 57 galaxies classified as Scd in the *Reference Catalogue of Bright Galaxies* (de Vaucouleurs and de Vaucouleurs 1964; BGC) were observed. Satisfactory spectra were obtained for 46 galaxies. These data were then combined with the synthesis data of Rogstad and Shostak as well as with data from a study of NGC 4244 by Huchtmeier (1973), to produce the present sample.

In § II the observational techniques are described and the spectra are presented. Derivation and listing of the profile parameters will be found in § III. In § IV the integral properties are derived; their significance is considered in § V.

II. OBSERVATIONS

All new observations were made using the NRAO 300-foot (91 m) transit telescope. The procedures were as described in Peterson and Shostak (1974).

In 1972 July, a preliminary observing run was undertaken using one feed of a four-feed receiver having a system temperature of ~ 150 K. Only the strongest emitters were observed with this equipment; all subsequent observations were made with a cryogenic, dual-feed parametric amplifier with a system temperature of ~ 50 K per channel. Spectral processing was in all cases performed using the Model III 384-channel autocorrelator. Bandwidths were either 5 or 10 MHz, giving spectral resolution after processing of 11 or 21 km s^{-1}.

All spectra are the combination of several scans, the average number of observations of a given source being three. Galaxy positions were taken from the BGC.

For many of the sources redshifts were unknown. In such cases a search in the velocity field was made, based on a redshift estimated from the angular size and

* Operated by Associated Universities, Inc., under contract with the National Science Foundation.

TABLE 1

UNDETECTED GALAXIES

NGC Number	Search Range ($km\ s^{-1}$)
237..........	500–4800*
1179..........	−800–2800†
3782..........	1400–3000
4025..........	1300–3000
4301..........	1700–3300
4571..........	600–2200
4701..........	1400–3000
4904..........	1100–2800‡
7156..........	1700–3300
7348..........	300–2000

* Probable detection at 4180 $km\ s^{-1}$.

† Weak (0.04 Jy) detection at 1750 $km\ s^{-1}$.

‡ Detected: 0.15 Jy at $\sim$1150 $km\ s^{-1}$ (off scale).

apparent magnitude of the galaxy. A listing of those galaxies which failed to provide satisfactory profiles is given in Table 1. A conservative estimate of the minimum detectable flux would be 0.05 Jy.

Over 80 percent of the galaxies observed produced measurable profiles, and therefore the principal selection effects on our sample are those inherent to the BGC.

Spectra of the well-detected galaxies are presented in Figure 1. All radial velocities are heliocentric.

III. LINE-PROFILE PARAMETERS

Those quantities which are directly derived from the H I spectra are listed in Table 2. Individual column entries are discussed below.

Column (*1*).—NGC or IC designation.

Column (*2*).—Systemic velocity with respect to the Sun. This is defined to be the midpoint of the profile, and therefore assumes gross symmetry of the rotation field of the galaxies. The uncertainty in these values depends on individual signal-to-noise ratios; the average uncertainty is ± 9 $km\ s^{-1}$.

Column (*3*).—Total line profile width ΔV. This is the velocity difference between points on the profile which are at $\sim$20 percent of the average flux level. A small correction for the filter width has been applied.

Column (*4*).—Profile integral. The area under each line profile has been determined by planimetry. Flux scale uncertainty ascribable to calibration error is no more than 15 percent. Before these integrals can be used to derive H I masses, correction must be made for the effect of the telescope beam; this correction is discussed in § IV.

IV. DERIVED QUANTITIES

By using the observed H I parameters in conjunction with published optical data, several large-scale physical properties of the galaxies can be derived. Table 3 lists these derived quantities; a detailed description of individual column entries follows:

Column (*1*).—NGC or IC designation.

Column (*2*).—Distance in Mpc. Good distance estimates are essential, as they are used to derive all the integral properties. Three sources of distances were considered for the present study: (1) group membership as determined by de Vaucouleurs (1974); (2) values listed by Gouguenheim (1969) based on criteria described by Bottinelli *et al.* (1968); and (3) redshift distances.

Thirteen of the galaxies are ascribed group membership by de Vaucouleurs. Distances for four others are given by Gouguenheim. Investigation of de Vaucouleurs's group distances shows them to be consistent

Table 2

Line Profile Parameters

(1) NGC or IC(*)	(2) $V_{\odot}$ ($km\ s^{-1}$)	(3) ΔV ($km\ s^{-1}$)	(4) $\int S dV$ ($Jy\ km\ s^{-1}$)
275[a]	1750	338	28.5
450	1761	204	29.1
672	409	299	148.8
895	2294	291	43.1
*239	903	149	84.3
1003	626	244	131.8
1042	1368	125	36.0
1337	1238	275	72.5
1376	4155	183	11.5
2541	561	224	110.4
2763	1889	228	16.7
3184	595	142	87.2
3206	1158	204	35.7
3319	744	236	69.6
3320	2331	309	16.6
3395[b]	1631	228	37.8
3423	1013	189	37.2
3556	699	339	138.0
3629	1508	244	22.5
3917	963	299	22.9
4144	263	165	42.0
4183	931	260	42.5
4189[c]	2101	292	17.2
4294[d]	359	244	24.8
4487	1037	228	26.7
4504	998	252	81.2
4517	1129	315	103.0
4559	816	260	217.0
4654	1037	315	45.9
4688	981	71	30.0
4731	1495	260	99.2
4808	778	236	52.0
4951	1180	271	32.6
4961	2535	228	13.5
5112	965	228	41.5
5468	2845	157	29.5
5474	273	63	87.5
5523	1047	283	45.3
5584	1635	212	27.6
5669	1371	220	39.7
6015	835	327	80.6
6070	2010	417	30.2
6118	1571	354	21.4
6503	62	196	113.2
7218	1662	283	20.0
7741	753	216	46.2
598[e]	-180	169	--
*342[e]	25	162	--
2403[e]	128	218	--
4244[f]	242	200	--
5457[e]	240	151	--
6946[e]	40	208	--

Notes to Table 2. a. Possibly confused by NGC274 (Arp 140). b. Multiple skirts in profile may result from confusion with NGC3396. c. Possibly confused with NGC4193. d. Confused with NGC4299. e. Data from Rogstad and Shostak (1972). f. Data from Huchtmeier (1973).

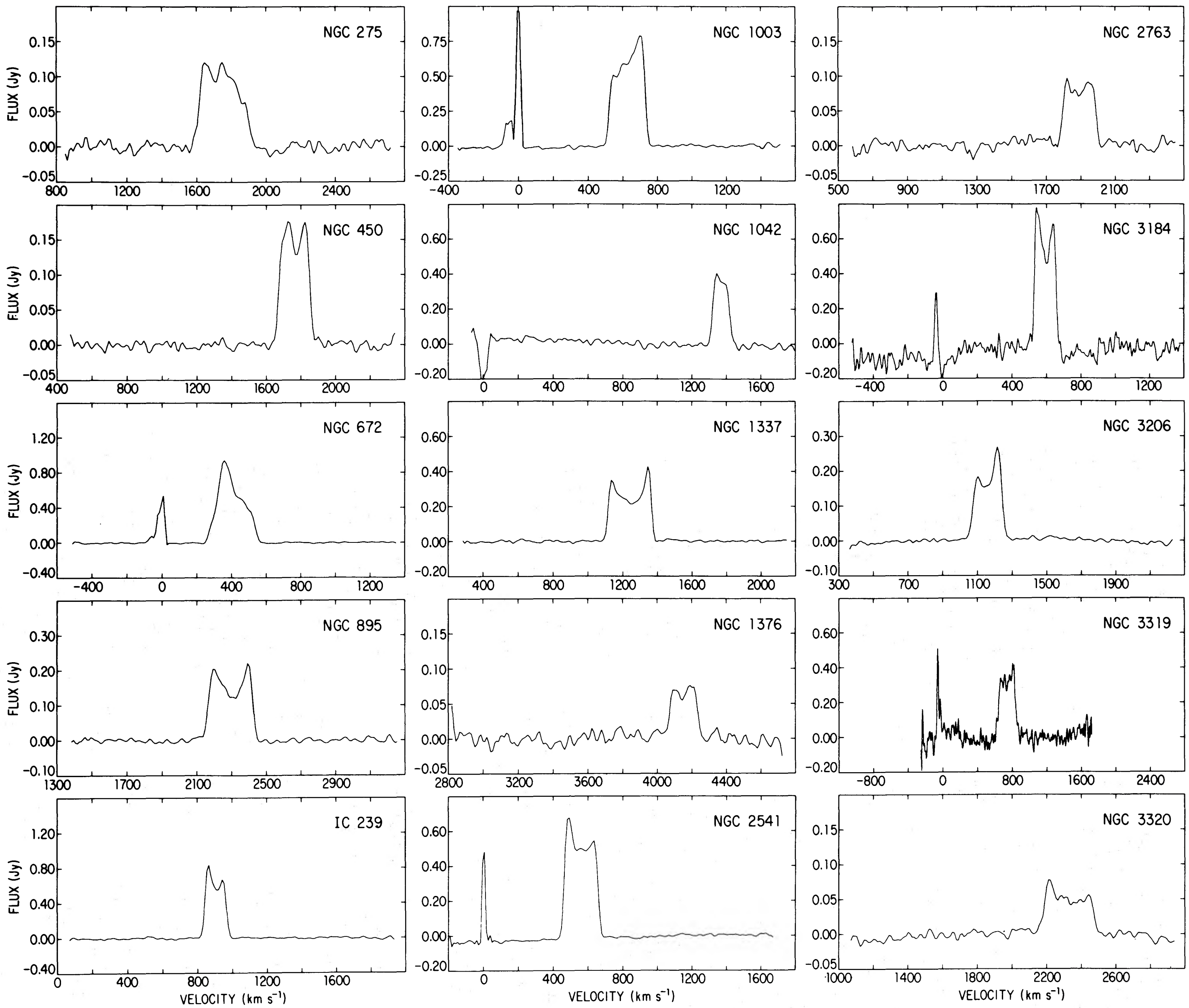

FIG. 1a

FIG. 1.—H I global profiles of Scd galaxies. For NGC 3184, 3319, 3556, 4517, 4688, and 4808, spectral resolution is 11 km s^{-1}. In all other cases it is 21 km s^{-1}. Velocities are heliocentric. Spikes near 0 km s^{-1} are caused by local H I.

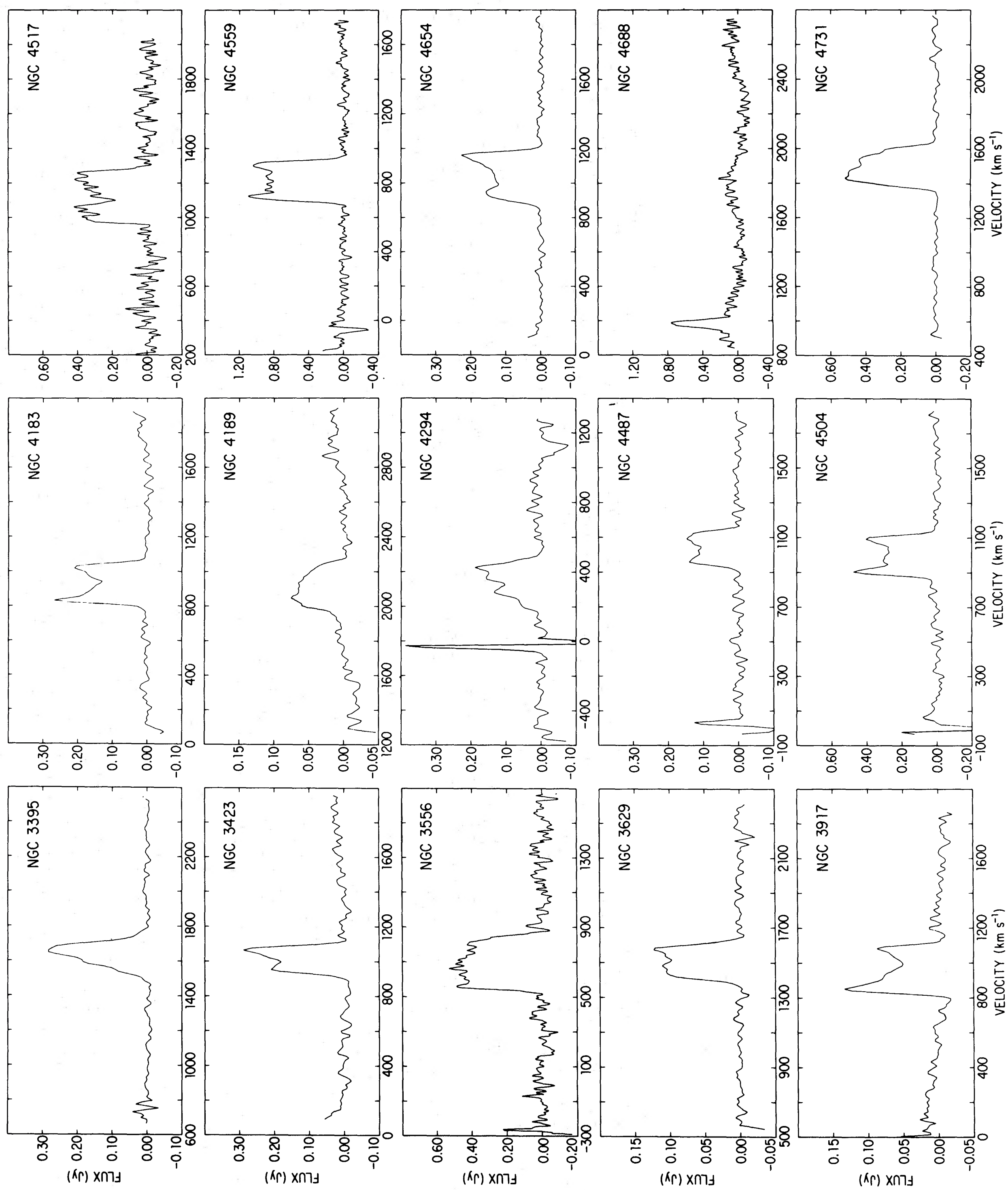

FIG. 1b

FIG. 1.—*Continued*

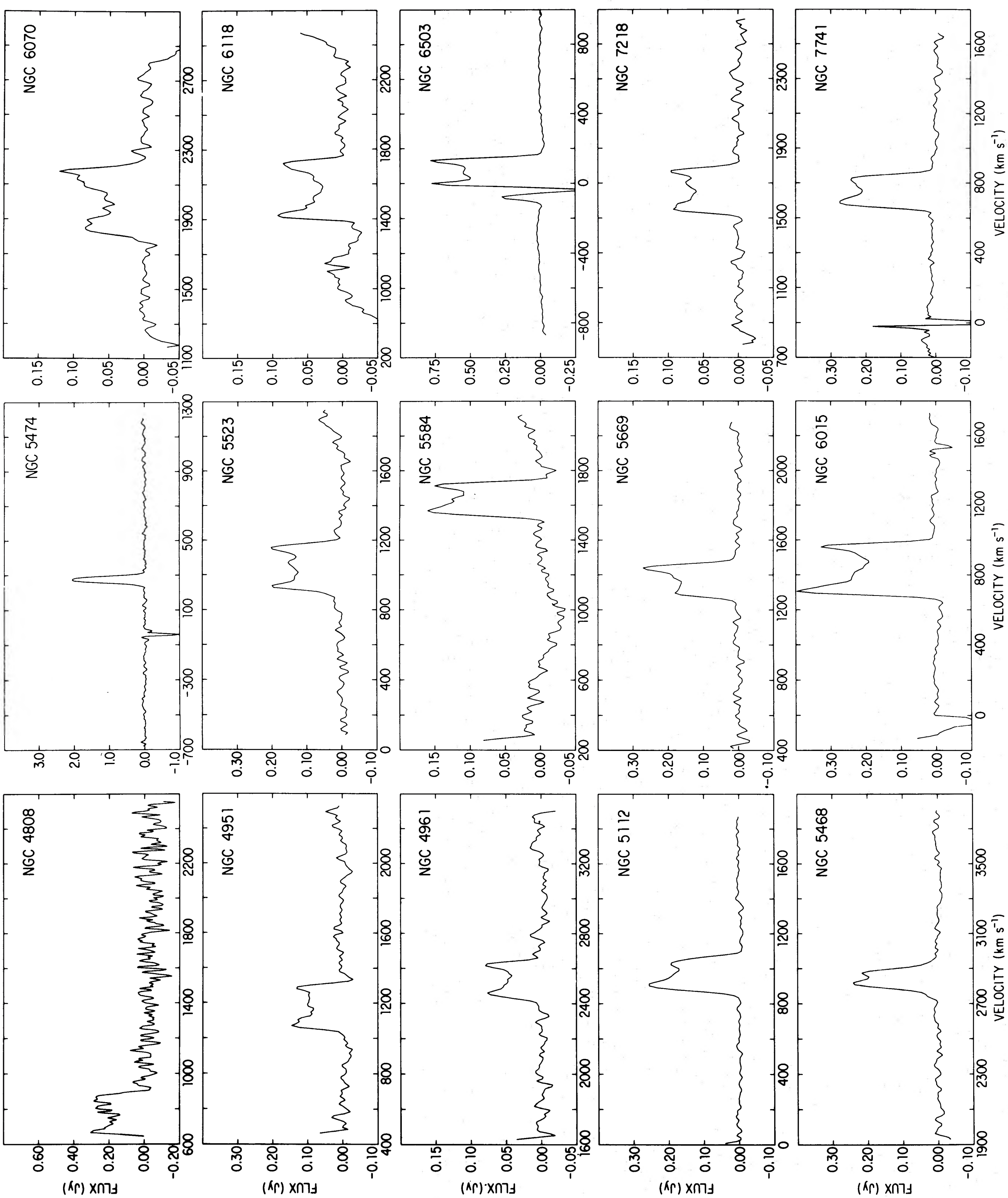

Fig. 1c

Fig. 1.—*Continued*

Table 3

Derived Properties

(1) NGC or IC(*)	(2) D (Mpc)	(3) i (deg.)	(4) θ_H (arcmin)	(5) $(B-V)_o$ (mags.)	(6) m_{pg} (mags.)	(7) ΔV_{True} (km s^{-1})	(8) M_{HI} ($10^9 M_\odot$)	(9) M_T ($10^9 M_\odot$)	(10) L_{pg} ($10^9 L_\odot$)	(11) M_{HI}/M_T	(12) M_{HI}/L_{pg} ($M_\odot/L_\odot$)	(13) M_T/L_{pg} ($M_\odot/L_\odot$)	(14) σ_{HI} $10^6 \odot$ kpc^{-2})	(15) σ_{MT} ($10^7 \odot$ kpc^{-2})	(16) σ_L ($10^7 \odot$ kpc^{-2})
275	33.3	46°	2!2		$12^m.57$	469	7.7	67.	15.	0.11	0.53	4.6	20.	23.	4.3
450	33.6	40	4.5		12.05	317	8.3	64.	24.	.13	.35	2.7	4.3	5.5	1.6
672	10.3	72	9.2	$0^m.59$	10.37	314	4.6	40.	11.	.12	.43	3.8	6.7	7.6	1.8
895	41.9	38	5.4		11.38	472	20.	213.	69.	.09	.28	3.1	6.4	5.9	2.1
*239	19.2	21	6.4	.72	11.04	415	8.6	90.	20.	.10	.43	4.6	9.0	8.5	2.0
1003	14.2	65	6.6	.57	10.81	269	7.0	29.	13.	.25	.52	2.1	4.9	12.	2.3
1042	24.6	16	6.7	.57	11.13	453	6.2	145.	30.	.04	.20	4.8	7.9	3.4	1.6
1337	21.4	72	5.9	.58	11.44	289	8.6	45.	17.	.19	.50	2.6	4.2	8.1	1.6
1376	74.6	25	2.8		12.22	433	16.	168.	101.	.09	.15	1.7	5.7	5.2	3.4
2541	10.8	63	7.5	.55	11.06	251	3.5	22.	6.2	.16	.57	3.5	5.0	8.1	1.4
2763	29.7	21	3.3	.63	11.82	636	3.6	166.	23.	.02	.16	7.2	26.7	5.8	3.7
3184	10.8	24	9,4	.64	9.96	349	3.3	52.	17.	.06	.20	3.1	7.7	4.9	2.5
3206	22.5	46	4.2		11.67	283	4.5	32.	15.	.14	.30	2.1	5.4	7.6	2.6
3319	13.6	63	7.6	.46	11.12	264	3.5	31.	9.3	.11	.38	3.3	4.3	4.9	1.3
3320	43.0	60	2.8		11.98	356	7.5	66.	42.	.11	.18	1.6	6.7	7.6	4.3
3395	29.0	52	3.0	.31	11.68	289	7.8	31.	25.	.25	.31	1.2	6.1	15.	5.0
3423	15.6	28	5.6	.46	11.14	402	2.4	60.	12.	.04	.20	5.0	12.0	4.8	2.4
3556	14.2	69	9.2	.63	9.88	363	8.1	74.	32.	.11	.26	2.3	6.4	7.0	2.8
3629	26.5	47	3.4		11.93	333	3.9	43.	17.	.09	.23	2.6	7.8	7.0	3.0
3917	19.0	78	5.6		11.03	305	2.1	42.	20.	.05	.11	2.2	5.6	2.8	2.6
4144	5.1	86	5.8		10.84	165	2.1	3.4	1.7	.62	1.2	2.0	5.9	36.	2.9
4183	17.9	90	5.5		11.94	260	3.5	28.	7.5	.12	.46	3.8	4.4	5.4	1.2
4189	36.7	30	3.3	.78	12.22	584	5.8	176.	25.	.03	.23	7.2	18.	5.9	2.5
4294	5.0	63	3.7	.54	11.94				.59						2.6
4487	16.1	46	5.8		11.04	316	1.8	40.	14.	.05	.13	2.8	6.9	3.2	2.4
4504	15.4	50	5.8		11.23	328	5.0	41.	11.	.12	.47	3.8	7.7	9.5	2.0
4517	18.3	85	11.1	.74	10.13	316	11.	87.	42.	.12	.26	2.1	3.1	3.9	1.5
4559	14.8	57	11.3	.47	9.83	310	15.	68.	36.	.22	.43	1.9	3.7	8.3	1.9
4654	17.7	47	5.0	.67	10.67	430	3.7	70.	24.	.05	.15	2.9	13.	7.0	4.5
4688	16.1	21	6.9		13.71	198	2.2	19.	1.2	.12	1.9	15.	2.3	2.7	.15
4731	24.8	76	7.6		10.33	267	16.	57.	64.	.29	.26	.90	2.4	7.0	2.7
4808	12.6	65	3.7		11.33	260	2.0	13.	6.5	.15	.31	2.0	9.4	14.	4.6
4951	19.2	71	4.0		11.58	286	3.0	27.	12.	.11	.24	2.2	6.8	7.4	3.0
4961	46.4	43	2.3	.46	13.53	334	7.1	50.	12.	.14	.60	4.2	6.8	9.7	1.6
5112	18.8	45	5.4	.47	12.00	322	3.8	45.	7.9	.08	.48	5.7	6.5	5.5	1.1
5468	50.5	17	4.0		11.70	536	19.	245.	75.	.08	.25	3.3	9.2	7.1	2.8
5474	7.7	21	7.1	.51	10.91	175	1.5	7.1	3.6	.21	.42	2.0	3.6	7.5	1.8
5523	20.1	78	4.8		11.85	289	4.6	34.	10.	.13	.44	3.3	5.5	7.3	1.6
5584	29.1	46	4.7		11.79	294	5.9	50.	23.	.12	.26	2.2	4.1	4.8	1.9
5669	25.2	48	5.2		12.20	296	6.5	49.	12.	.13	.55	4.1	4.3	5.7	1.0
6015	19.1	65	5.4	.60	11.03	360	7.5	57.	20.	.13	.38	2.9	8.1	11.	2.8
6070	37.8	62	4.4	.71	11.57	472	11.	159.	47.	.07	.23	3.4	8.5	5.7	2.5
6118	29.7	65	5.7	.86	11.68	390	4.9	110.	26.	.04	.18	4.2	5.7	2.5	1.4
6503	5.7	72	9.1	.69	9.79	206	1.1	9.5	5.6	.11	.19	1.7	5.2	5.9	3.1
7218	32.5	63	3.1		11.95	317	5.1	43.	25.	.12	.21	1.8	6.4	7.5	3.6
7741	18.0	58	6.4	.65	10.98	254	3.9	32.	18.	.12	.21	1.7	3.6	4.5	2.1
598	0.72	55	75.	.55	5.73	206	1.6	9.7	3.7	.17	.44	2.6	5.0	8.5	1.9
*342	4.50	25	39.		7.07	383	15.	110.	42.	.13	.35	2.6	5.3	7.1	2.0
2403	3.25	60	26.	.53	8.25	251	3.5	22.	7.4	.16	.47	3.0	4.9	7.7	1.6
4244	3.80	86	13.	.51	9.53	200	7.2	8.6	3.1	.84	2.3	2.7	5.1	43.	1.9
5457	6.90	22	28.	.50	8.29	403	18.	131.	32.	.14	.57	4.1	5.5	7.7	1.3
6946	10.10	30	19.	.82	7.89	416	21.	144.	100.	.15	.21	1.4	5.6	8.3	3.9

with a value $H_0 = 100$ km s^{-1} Mpc^{-1}, as are the relevant Gouguenheim distances.

To ascertain the desirability of using nonredshift distances, we performed a simple test. Published data on galaxies suggest that the distance-dependent ratio mass to luminosity M_T/L_{pg} is invariant for all spirals. This quantity was computed (see below) for the 17 systems having listed nonredshift distances, and recomputed assuming redshift distances. Although the average values of M_T/L_{pg} were identical for both groups, the dispersion was reduced by more than a factor of 2, from 3.4 to 1.6 (solar units), when redshift distances were used. Consequently, we have elected to use only redshift distances for the present work. Heliocentric velocities were corrected to the rest frame of the Local Group according to de Vaucouleurs and de Vaucouleurs (1964), and distances derived assuming $H_0 = 55$ km s^{-1} Mpc^{-1}. The five mapped galaxies taken from Rogstad and Shostak (1972) have distances given by Tammann (1972) which are consistent with this choice for H_0.

Column (*3*).—Inclination to sky plane in degrees. These were taken from Danver (1942), or derived from the axis ratios given by Holmberg (1958) or the BGC according to

$$\cos i = \{[(b/a)^2 - 0.04]/0.96\}^{1/2} .$$

The above relation assumes an intrinsic axial ratio of 0.2.

Column (*4*).—Holmberg diameter in arcmin. When available, Holmberg's (1958) photometric diameters were used; otherwise, values listed in de Vaucouleurs and de Vaucouleurs (1964) were converted to the Holmberg system according to $\theta_H = 1.55\theta_{BGC}$. This conversion is given by Heidmann, Heidmann, and de Vaucouleurs (1972; hereafter designated H^{2}V).

A dependence of measured photometric diameter on inclination is expected simply due to the changes in path length of the light through a galaxy of finite thickness, and indeed the uncorrected values of θ_H show a marked average increase with inclinations. H^{2}V consider a variation of the form

$$\frac{\partial \log \theta_H}{\partial \log (b/a)} = -c ,$$

where b/a is the ratio of apparent minor to major axes and c is a constant. A least-squares solution for the 46 detected galaxies of the present sample yielded $c = 0.4$. However, the effect is expected to be overestimated due to selection effects. Edge-on systems, being more difficult to classify, will be underrepresented. A solution employing linear, rather than angular, diameters is less susceptible to such effects, assuming our sample is complete to a given apparent magnitude. A least-squares fit yields $c = 0.2$, in agreement with the value found by H^{2}V for all types when using BGC diameters. Note that most of the diameters used in the present study, although on the Holmberg system, are taken from the BGC.

The diameters listed in column (4) have been corrected according to $\theta_{corr} = \theta(b/a)^{0.2}$.

Column (*5*).—Color $(B - V)_0$ from the BGC.

Column (*6*).—Corrected apparent photographic magnitude. The sources of the magnitude measures, in decreasing order of preference, were (1) Holmberg (1958); (2) $B(0)$ values from the BGC; (3) Zwicky *et al.* (1961); and (4) corrected Harvard magnitudes m_c from the BGC. All measures were first converted to the Holmberg system. The Zwicky *et al.* magnitudes were corrected according to Holmberg (1969), and $B(0)$ and m_c magnitudes according to

$$m_H = 0.99 m_{BGC} - 0.24$$

(Roberts 1969).

Two further corrections have been applied to the listed magnitudes. The first is a correction for galactic obscuration, and is taken to be 0.25 csc $|B|$, where B is the galactic latitude of the object. The second is the correction for internal absorption. A usual procedure has been to correct the magnitudes to a face-on ($i = 0°$) aspect using the data of Holmberg (1958). Holmberg computed surface brightness according to

$$S = m_{pg} + 5 \log \theta_H (\text{mag arcmin}^{-2}) ,$$

and observed how this quantity varied with inclination. The procedure has been repeated for the present data by computing S and plotting it versus axial ratio (b/a) (Fig. 2). Also plotted in the figure is the curve taken from Holmberg and average values (with errors) of the present data. The lower absorption curve is a consequence of our correction of diameters for inclination effects (see H^{2}V).

The magnitudes in column (6) have been corrected for internal absorption using the newly derived absorption curve.

Column (*7*).—ΔV_{true}, profile widths corrected to the plane of the galaxy. The mean value, excluding confused systems, is $\Delta V_{true} = 328$ km s^{-1}, with $\sigma = 94$ km s^{-1}. This agrees with Brosche's (1971) value for this type, although the dispersion is great enough to encompass the average values for all spirals.

Column (*8*).—Hydrogen mass $M_{H\,I}$, assuming the gas to be optically thin. A correction for attenuation by the 10′ telescope beam was made. A radial H I distribution which was the average of those found by Rogstad and Shostak (1972) was assumed, and the beam corrections were computed as a function of Holmberg diameter and inclination. The corrections are not overly sensitive to the model adopted, and in no case exceeded 38 percent, the average correction being 12 percent.

No correction has been made for optical depth effects. Roberts's (1969) data show a decrease of a factor of 2 in the ratio $M_{H\,I}/L_{pg}$ for galaxies with axial ratios of $(b/a) \leq 0.25$, presumably caused by an increase in the optical depth of H I with greater inclination. However, any tabulation of $M_{H\,I}/L_{pg}$ which does not account for the diameter-inclination effect discussed earlier will include a dependence

$$L_{pg} \propto (b/a)^{-5c} .$$

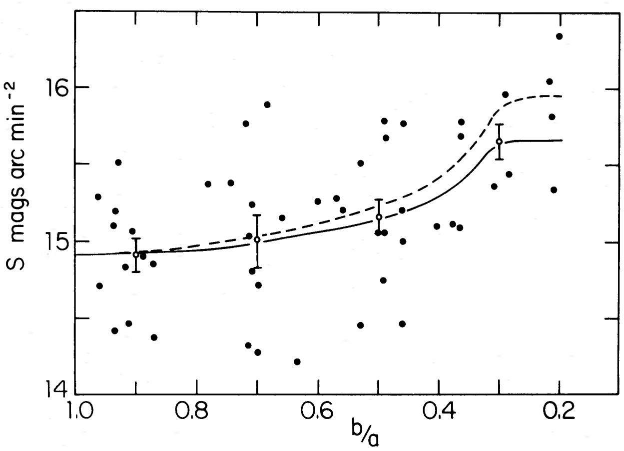

FIG. 2.—Photographic surface brightness S versus observed axial ratio (b/a). Interval averages, together with errors, are shown. *Solid curve*, adopted internal absorption dependence used to derive absolute magnitudes in this paper; *dotted curve*, from Holmberg's (1958) study of late spirals.

A value for c of as little as 0.1 would account for the effect found by Roberts, who made no diameter-inclination corrections. The value for c found here is 0.2. The values of $M_{\rm H\,I}/L_{\rm pg}$ in Table 3 exhibit no dependence on axial ratio. Any decrease of this ratio at high inclinations ($b/a \leq 0.25$) is less than ~ 30 percent. Therefore the average H I optical depth perpendicular to the galactic plane must be < 0.2.

Column (*9*).—Total masses M_T computed according to

$$\frac{M_T}{M_\odot} = 4.25 \times 10^3 \Delta V^2 \theta_{\rm H} D\,,$$

where the units of Tables 2 and 3 apply. This formula derives from Brandt (1960) and is the one used by Roberts (1968), assuming a shape parameter $n = 3$ and turnover radius $= \theta_{\rm H}/6$. We have adopted this formulation in order to retain compatibility with earlier studies. It should be emphasized that these masses are considerably extrapolated: only 20–50 percent of the total mass given by Brandt's formulation lies within the Holmberg radius and can be considered observed. Since all models give masses which scale as $\theta \Delta V^2$, the listed masses can be converted to other systems by simple rescaling. For example, the indicative masses derived by Nançay observers are related via $M_i = 2.05 M_T$. If we adopt rotation curves of the form found by Rogstad and Shostak, for which $n = 1$ and the turnover radius $= 0.3\theta_{\rm H}$, we find masses which are 4.05 times those given in column (9).

Column (*10*).—Absolute photographic luminosities, $L_{\rm pg}$.

Column (*11*).—Fractional H I mass, $M_{\rm H\,I}/M_T$.

Column (*12*).—Ratio of H I mass to luminosity, $M_{\rm H\,I}/L_{\rm pg}$. Note that this quantity and the surface densities (below) are not dependent on distance.

Column (*13*).—Mass-to-luminosity ratio, $M_T/L_{\rm pg}$.

Column (*14*).—H I surface density, $\sigma_{\rm H\,I}$, defined by $M_{\rm H\,I}/\pi(\theta_{\rm H}/2)^2$. This mixed quantity assumes a fixed relationship between the optical and H I diameters.

Column (*15*).—Total mass surface density σ_M, defined analogously to $\sigma_{\rm H\,I}$.

Column (*16*).—Luminosity surface density, σ_L, defined analogously to $\sigma_{\rm H\,I}$.

V. DISCUSSION

a) *Profile Shapes*

The profiles of Figure 1 display a characteristic double peak. The average ratio of peak flux to the flux at the systemic velocity is 1.4. Model studies (J. Rubin, 1973) indicate that the peaks are caused by H I in the outer regions of the galaxy where nearly constant circular velocities obtain. We infer that the relatively flat rotation curves ($n = 1$) found for five Scd galaxies by Rogstad and Shostak (1972) are typical of the majority of spirals of this type. Total masses for these objects are consequently uncertain, as discussed above. The possible absence of H I in the central regions, as observed in several spirals (e.g., Roberts 1966; Rogstad and Shostak 1971), only slightly alters the ratio of peak-to-systemic velocity flux, and cannot be deduced from the profile shapes alone.

The morphology of the profiles is so regular that a major departure from the characteristic shape is observed only in case of a confusing, second galaxy in the telescope beam. Confused spectra are noted in Table 2.

b) *Integral Property Ratios*

Histograms of the principal integral properties are given in Figure 3. Mean logarithmic values of these quantities, together with their dispersions, are listed in Table 4. These values are based on the 48 unconfused objects of Tables 2 and 3. In general, they are in reasonably good agreement with those of Roberts (1969) and Balkowski (1973) when account is made of the different distance scales used. The largest discrepancy is for the distance independent quantity $M_{\rm H\,I}/L_{\rm pg}$, which is significantly less for the present

TABLE 4

MEAN LOGARITHMIC VALUES AND DISPERSIONS OF INTEGRAL PROPERTIES

Quantity	Mean Value (dispersion)
$M_{\rm H\,I}/M_T$:	-0.94 (solar units) (0.28)
$M_{\rm H\,I}/L_{\rm pg}$:	-0.48 (solar units) (0.27)
$M_T/L_{\rm pg}$:	0.45 (solar units) (0.21)
$\sigma_{\rm H\,I}$:	0.83 ($10^6{}_\odot$ kpc^{-2}) (0.23)
σ_{MT}:	0.77 ($10^7{}_\odot$ kpc^{-2}) (0.18)
σ_L:	0.35 ($10^7{}_\odot$ kpc^{-2}) (0.18)

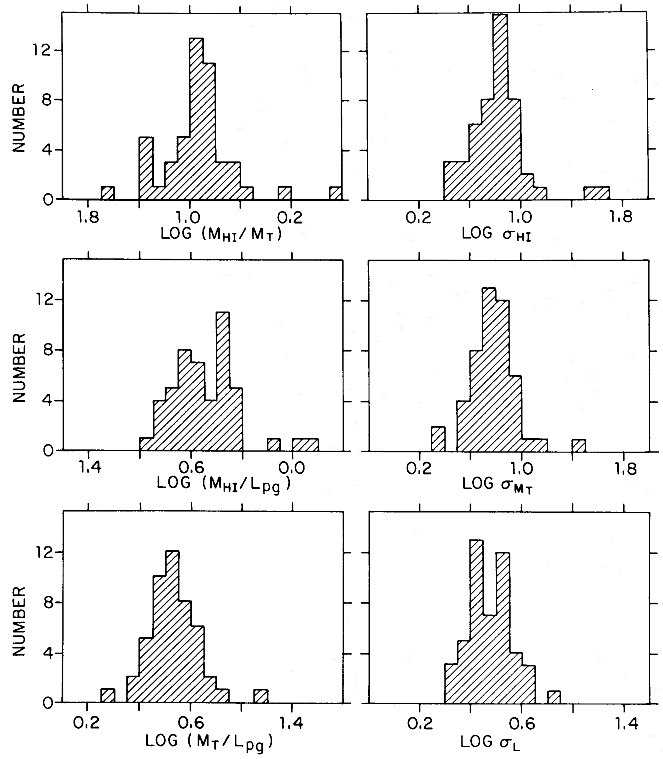

FIG. 3.—Histograms of integral property ratios for unconfused Scd galaxies. Quantities are expressed in solar units except $\sigma_{\rm H\,I}(10^6\ M_\odot\ {\rm kpc}^{-2})$ and σ_{M_T}, $\sigma_L(10^7\ M_\odot\ {\rm kpc}^{-2})$.

sample. Furthermore, the dispersions in all quantities are less than in preceding studies.

In particular, it is interesting to note that dispersions in the distance-dependent ratios ($M_{\rm H\,I}/M_T$, $M_T/L_{\rm pg}$) are not definitely greater than for distance-independent quantities. The deduced limit on dispersion introduced by distance errors is 0.15 in the log. Our decision, then, to assign all distances on the basis of recession velocity alone results in an estimate of the average precision of this method of better than 0.8 mag in the distance modulus.

To what extent are the listed dispersions of Table 4 intrinsic to the sources? An estimate can be made by restricting ourselves to those galaxies for which magnitudes and diameters were measured photometrically (Holmberg 1958). These optical parameters are otherwise the least accurate quantities used in the calculation of integral properties. For the photometric subgroup (18 objects), dispersions were reduced by ~ 0.08, although average values remained unchanged. The intrinsic dispersions, therefore, are likely to be less than 0.2, or ± 50 percent. For comparison, the ratios $M_{\rm H\,I}/M_T$ and $M_{\rm H\,I}/L_{\rm pg}$ vary by a factor of ~ 3 when going from type Sa to Sm (Roberts 1969).

With the reduced dispersions found here, the desirability of a second parameter, other than Hubble class, to define the quantities of Table 4 is uncertain. Bottinelli and Gouguenheim (1974) summarize the arguments for a second parameter, suggesting the initial gas density as candidate. This quantity is reflected in the galaxy's color, dependent on the initial star formation rate and therefore the gas density (Searle, Sargent, and Bagnuolo 1973). The reddest galaxies, presumably the most efficient converters of gas into stars, should have the lowest fractional H I masses. The 27 unconfused galaxies of Tables 2 and 3 having measured colors fail to show such a relation. Possibly, replenishment of the interstellar environment

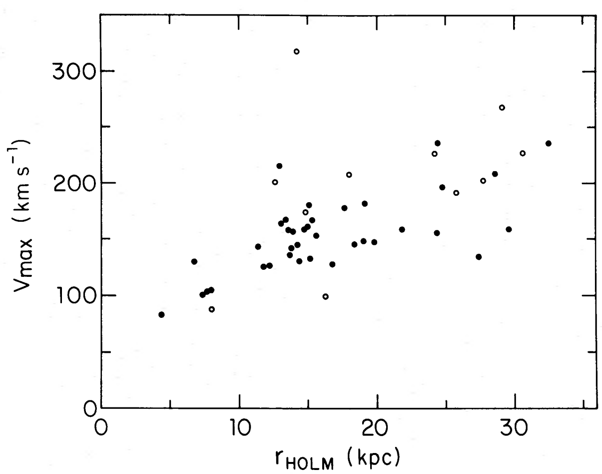

FIG. 4.—Maximum rotation velocity $V_{\rm max} = \Delta V/2 \sin i$ versus Holmberg radius in kpc. A least-squares fit yields $V_{\rm max} \approx r_{\rm Holm}^{0.44}$. The open circles represent galaxies with inclinations less than 30°.

has occurred via mass loss from old stars. If the rates cited by Tinsley (1973) are correct, a significant fraction of presently observed H I could be recycled.

c) Dependence of V_{max} on Radius

Rogstad and Shostak (1972) found a linear correlation between $V_{max} = \Delta V/2 \sin i$ and Holmberg radius. In Figure 4 is shown the relationship given by the present data. The open circles represent galaxies with inclinations less than 30°, and consequently less reliable values of V_{max}. A fit of the form

$$V_{max} = K r_H{}^m$$

yields $K = 47$ km s^{-1} and $m = 0.44$. The total mass therefore scales approximately as $r_H{}^2$. If a substantial halo mass existed, we would expect $M_T \sim r_H{}^3$. The present result implies a two-dimensional mass distribution, with the assumption that all objects have similar rotation curves.

VI. CONCLUSIONS

Data are presented for 52 Scd galaxies which exhibit a $\sim$100:1 range of H I and total masses. Their integral property ratios are well defined and have observed dispersions of $\sim \pm 80$ percent. The intrinsic dispersions are probably less than ± 50 percent. The lack of measurably greater dispersion in the distance-dependent ratios relative to distance-independent quantities indicates that the distance moduli, established solely from redshifts, are on average accurate to ± 0.8 mag.

No indication of optical depth effects with inclination are observed. The average H I optical depth perpendicular to the plane of the galaxies must be <0.2.

A relationship between V_{max} and r_H suggests that the total mass grows as $\sim r_H{}^2$.

REFERENCES

Balkowski, C. 1973, *Astr. and Ap.*, **29**, 43.
Bottinelli, L., Gouguenheim, L., Heidmann, J., and Heidmann, N. 1968, *Ann. d'Ap.*, **31**, 205.
Bottinelli, L., and Gouguenheim, L. 1974, *Astr. and Ap.*, **33**, 269.
Brandt, J. C. 1960, *Ap. J.*, **131**, 293.
Brosche, P. 1971, *Astr. and Ap.*, **13**, 293.
Danver, C. G. 1942, *Ann. Obs. Lund.*, No. 10, p. 1.
de Vaucouleurs, G. 1974, Vol. **9** of *Stars and Stellar Systems* (Chicago: University of Chicago Press), in preparation.
de Vaucouleurs, G., and de Vaucouleurs, A. 1964, *Reference Catalogue of Bright Galaxies* (Austin: University of Texas).
Gouguenheim, L. 1969, *Astr. and Ap.*, **3**, 281.
Heidmann, J., Heidmann, N., and de Vaucouleurs, G. 1972, *M.N.R.A.S.*, **75**, pp. 85, 105, and 121.
Holmberg, E. 1958, *Medd. Lunds. Astr. Obs.*, II, No. 136.
———. 1969, *Ark. f. Astr.*, **5**, 305.
Huchtmeier, W. 1973, *Astr. and Ap.*, **23**, 93.
Peterson, S. D., and Shostak, G. S. 1974, *A.J.*, **79**, 767.
Roberts, M. S. 1966, *Ap. J.*, **144**, 639.
———. 1968, *A.J.*, **73**, 945.
———. 1969, *ibid.*, **74**, 859.
Rogstad, D. H., and Shostak, G. S. 1971, *Astr. and Ap.*, **13**, 99.
———. 1972, *Ap. J.*, **176**, 315.
Rubin, J. 1973, private communication.
Searle, L., Sargent, W. L. W., and Bagnuolo, W. G. 1973, *Ap. J.*, **179**, 427.
Tammann, G. A. 1972, private communication.
Tinsley, B. M. 1973, *Ap. J.*, **186**, 35.
Zwicky, F., *et al.* 1961–1968, *Catalogue of Galaxies and Clusters of Galaxies* (Pasadena: California Institute of Technology).

G. S. SHOSTAK: 2200 Ben Franklin Pkwy., E907, Philadelphia, PA 19130